Tracing of particulate organic C sources across the terrestrial-aquatic continuum, a case study at the catchment scale (Carminowe Creek, South West England)

M. Glendell[1*], R. Jones[2], J.A.J. Dungait[3], K. Meusburger[4], A.C. Schwendel[5], R. Barclay[2], S. Barker[6], S. Haley[2], T.A. Quine[2], J. Meersmans[7]

(1) The James Hutton Institute, Craigiebuckler, Aberdeen AB15 8QH, UK

(2) University of Exeter, Geography - College of Life and Environmental Sciences, Exeter EX4 4RJ, UK

(3) Sustainable Agriculture Science, Rothamsted Research, North Wyke, Okehampton, Devon, EX20 2SB, UK

(4) Environmental Geosciences, University of Basel, Bernoullistrasse 30, 4056 Basel, Switzerland

(5) School of Humanities, Religion & Philosophy, York St John University, Lord Mayor's Walk, York, YO31 7EX, UK

(6) Environment and Sustainability Institute, University of Exeter, Penryn Campus, Penryn, Cornwall TR10 9FE

(7) School of Water, Energy and Environment, Cranfield University, Bedford, MK43 0AL, UK

* Corresponding author: The James Hutton Institute, Craigiebuckler, Aberdeen AB15 8QH, Scotland, UK, Miriam.Glendell@hutton.ac.uk, tel: +44(0)1224 395 320, fax: +44 (0)844 928 5429

Abstract

Soils deliver crucial ecosystem services, such as climate regulation through carbon (C) storage and food security, both of which are threatened by climate and land use change. While soils are important stores of terrestrial C, anthropogenic impact on the lateral fluxes of C from land to water remains poorly quantified and not well represented in Earth system models. In this study, we tested a novel framework for tracing and quantifying lateral C fluxes from the terrestrial to the aquatic environment at a catchment scale. The combined use of conservative plant-derived geochemical biomarkers *n*-alkanes and bulk stable $\delta^{13}C$ and$\delta^{15}N$ isotopes of soils and sediments within an inter-disciplinary framework allowed us to distinguish between particulate organic C sources from different land uses (i.e. arable and temporary grassland *vs*. permanent grassland *vs*. riparian woodland *vs*. river bed sediments) ($p<0.001$), showing an enhanced ability to distinguish between land use sources as compared to using just biomarkers alone. The terrestrial-aquatic proxy (TAR) ratio derived from *n*-alkane signatures indicated an increased input of terrestrial-derived organic matter (OM) to lake sediments over the past 60 years, with an increasing contribution of woody vegetation over time. This may be related to agricultural intensification, leading to enhanced soil

erosion, but also an increase in riparian woodland that may disconnect OM inputs from arable land uses in the upper parts of the study catchment. Spatial variability of geochemical proxies showed a close coupling between OM provenance and riparian land use, supporting the new conceptualization of river corridors (active river channel and riparian zone) as critical zones linking the terrestrial and aquatic C fluxes. Further testing of this novel tracing technique shows promise in terms of quantification of lateral C fluxes as well as targeting of effective land management measures to reduce soil erosion and promote OM conservation in river catchments.

Keywords: lateral carbon fluxes, sediment fingerprinting, biomarkers, *n*-alkanes, bulk stable ^{13}C and ^{15}N isotopes

1. Introduction

Soils are critical to human wellbeing and deliver crucial ecosystem services, including climate regulation and food security (Adhikari and Hartemink, 2016; Mouchet et al., 2016). However, since the onset of agriculture, human activities have greatly altered soil processes at a global scale, with consequences for the essential functions of soils to sequester and store carbon (C), recycle nutrients and resist soil erosion (Amundson et al., 2015). As soils represent the largest terrestrial store of organic C, more than three times as much as either the atmosphere or terrestrial vegetation (Schmidt et al., 2011), these anthropogenic interventions have also impacted the scale of the lateral fluxes of C from land to inland waters (Lauerwald et al., 2015; Tian, 2015; Wohl et al., 2017).

However, the fluxes of C from land to ocean remain poorly quantified and not fully accounted for in the current generation of Earth system models (Regnier et al., 2013). While over the past decade, the understanding of rivers has been revised from 'inert pipes' simply transporting C from lad to the ocean to 'active agents', which play a crucial role in receiving, transporting and processing C equivalent to net terrestrial primary production in their watersheds (Aufdenkampe et al., 2011; Battin et al., 2009; Cole et al., 2007; Wohl et al., 2017)., the magnitude, spatiotemporal patterns and controls on C fluxes from land to ocean remain poorly quantified (Regnier et al., 2013; Wohl et al., 2017). While there is a growing understanding of the magnitude of global C exports from rivers to the ocean (Li et al., 2017; Ludwig et al., 2011; Tian et al., 2015), estimates of CO_2 evasion from inland waters (Lauerwald et al., 2015; Raymond et al., 2013) and sediment burial in aquatic ecosystems (Maavara et al., 2017; Tranvik et al., 2009) are still uncertain. However, the largest uncertainties are associated with the scale of the total lateral C fluxes from land to inland waters, with recent research suggesting that previous estimates may have largely over-estimated C accumulation in terrestrial ecosystems (the terrestrial C sink) due to under-estimation of this lateral C export (Nakayama, 2017). Therefore, there is a need to better understand the scale of the anthropogenic impact on these lateral C fluxes from land to water (Regnier et al., 2013; Wohl et al., 2017), as well as the processes involved in the loss and preservation of C along the terrestrial-aquatic continuum (Marín-Spiotta et al., 2014), to

properly represent these processes and predict the present and future contribution of aquatic C fluxes to the global C budget (Aufdenkampe et al., 2011; Battin et al., 2009; Cole et al., 2007; Regnier et al., 2013).

Over the past decades, the awareness of the importance of soils in the functioning of many vital ecosystem services, including climate change mitigation, food security, water resource management and flood protection has greatly increased (Schroter et al., 2005). Nevertheless, in many parts of the world where soil erosion rates exceed soil production, the sustainable provision of these ecosystem services is under pressure (Alewell, et al., 2015; Amundson et al., 2015; Panagos et al., 2015; Verheijen et al., 2009). The intensification of agriculture, particularly over the past 60 years, has led to an exponential increase in sediment and organic matter (OM) fluxes within agricultural catchments (Glendell and Brazier, 2014; Graeber et al., 2015), with important consequences for on-site impacts, such as soil productivity, and off-site impacts, in terms of nutrient pollution and sedimentation of water bodies (Tilman et al., 2002). Hence, conservation of soil organic matter (SOM; which contains ~60% SOC) remains critical for sustaining soil productivity and food security in a changing world (Amundson et al., 2015) and for mitigating the acknowledged wide-scale impacts of enhanced sedimentation and associated nutrient pollution on the ecological status of water bodies and drinking water quantity and quality (Bilotta and Brazier, 2008; Glendell et al., 2014a; Rickson, 2014; Schoumans et al., 2014).

Tracing and quantifying the sources of sediment and particulate organic C in the fluvial environment is, therefore, key to supporting sustainable land management decisions and maintaining ecosystem services. To date, most tracing techniques to apportion sediment sources in fluvial environments applied in river management studies have used physical sediment characteristics, geochemical properties, fallout radionuclides or mineral magnetic properties. However, these tracers are not able to distinguish sources between specific land uses, which are essential to inform mitigation measures and catchment management (Guzman et al., 2013; Owens et al., 2016; Smith et al., 2015; Walling, 2013). Conversely, examination of the provenance of sediment-bound OM using plant-specific biomarkers has been established in paleo-ecological and marine sciences for some time (e.g. Galy et al., 2011; Meyers and Lallier-Vergès, 1999; Meyers, 2003; Tolosa et al., 2013; Zech et al., 2012). While a number of studies to date have sought to apply one or more biomarkers to understand lateral C dynamics at the continental margins (e.g. Feng et al., 2015; Galy et al., 2011; Tao et al., 2016), few studies have applied this approach to inland waters, especially headwaters, which may cumulatively play an important role in lateral C export due to their spatial extent and close terrestrial – aquatic coupling. Therefore the application of biomarkers, especially aliphatic (saturated straight-chained) compounds such as *n*-alkanes (Chen et al., 2016, 2017; Cooper et al., 2015; Puttock et al., 2014) and *n*-carboxylic acids (fatty acids) (Alewell et al., 2016; Blake et al., 2012; Reiffarth et al., 2016), is now being examined as a new potential tool for attribution of sediment and C provenance in river catchments, with a potential to attribute organic matter sources to specific land uses, such as forest, arable and pasture.

N-alkanes are naturally occurring hydrocarbons which are relatively recalcitrant and more resistant to microbial decomposition than other functionalized plant-derived lipids, e.g. fatty

acids or sterols (Ranjan et al., 2015). They are vegetation-specific neutral lipids derived from plant waxes with different numbers of C atoms in the aliphatic molecule that are indicative of different provenances of OM (Eglinton, 1962). In general, long-chain (C_{27}-C_{31}) *n*-alkanes are derived from epicuticular plant waxes of terrestrial plants (Galy et al., 2011; Puttock et al., 2014), medium chain-length (C_{21}-C_{25}) *n*-alkanes are produces by lower plants and aquatic macrophytes (Fang et al., 2014; Meyers, 2003; Tolosa et al., 2013), while short chain-length (C_{15}-C_{19}) *n*-alkanes are typically derived from aquatic algae (Meyers, 2003). Both individual *n*-alkanes as well as different chain-length ratios have been used in paleo-ecological studies to attribute OM sources over decadal to millennial timescales (Ranjan et al., 2015; Zech et al., 2013, 2012). As *n*-alkane signatures are altered by land use change, they are ideally suited to track changing OM sources from eroded soils and sediments over time (Chen et al., 2016).

With these naturally occurring biomarkers (and their compound-specific isotopic signatures where vegetation sources with contrasting $\delta^{13}C$ values are evident) emerging as the new potential tools for tracing of SOM in catchment studies, a key challenge lies in establishing their effectiveness to act as land-management specific tracers of fluvial OM over decadal timescales (Alewell et al., 2016; Cooper et al., 2015). As these new techniques are still in their infancy (Owens et al., 2016) and require further development and testing, in this work we aim to investigate the suitability of *n*-alkane biomarkers within an inter-disciplinary context, beyond the traditional confines of soil science alone (Brevik et al., 2015; Owens et al., 2016; Smith et al., 2015).

Therefore, this pilot study aims to evaluate the combined use of *n*-alkanes, bulk stable $\delta^{13}C$ and $\delta^{15}N$ isotopes and their ratios (Collins, et al., 2014, 2013; Meyers and Lallier-Vergès, 1999; Meyers, 2003; Ranjan et al., 2015) to advance the current understanding of the temporal variability of lateral C fluxes from the terrestrial to the aquatic ecosystem in relation to changing land management practices, over the past century. Our aims were to i) test the ability of conservative *n*-alkane biomarkers and soil and sediment bulk stable $\delta^{13}C$ and $\delta^{15}N$ isotopes to distinguish between terrestrial and aquatic OM sources, ii) understand the impact of land use on the spatial variability of OM provenance in river bed sediments and iii) on OM accumulation in lake bed sediments, iv) test a methodology for quantifying the temporal variability and the magnitude of lateral C fluxes from land to water at catchment scales.

2. Material and Methods

2.1 Study site

The Carminowe Creek study catchment, located in southwest England (50°4' W 5°16'), covers c. 4.8 km^2 at an altitude range of 0-80 m above sea level (Fig. 1). The catchment outlet drains into a large freshwater lake Loe Pool (50 ha) that is separated from the Atlantic Ocean by a natural shingle barrier, thus creating a relatively closed natural hydrological system. The study catchment comprises two main streams (Northern and Southern subcatchments) with a joint outlet into the south-western branch of Loe Pool. The average total annual rainfall is

approximately 1000 mm and mean annual temperature is approximately 11°C (http://www.metoffice.gov.uk/public/weather/climate/). Bedrock geology comprises silt-, sand- and mudstone (http://mapapps.bgs.ac.uk/geologyofbritain/home.html), which is overlaid by freely draining loamy soils (Soil Survey of England and Wales, 1983). Land use on the catchment plateaux is dominated by cropland in rotation of arable crops and temporary grassland (also referred to as grass ley), while permanent grassland is found on steeper hillslopes, with riparian vegetation (mostly wet woodland dominated by willow *Salix sp.*, alder *Alnus glutinosa* and wet grassland) located in the riparian zone within the river corridor.

2.2 Field sampling

78 soil cores were taken 14 hillslope transects across the two sub-catchments (8 cm diameter, depth 0-15 cm), covering the topographic sequence from plateaux, convex, steep slope, concave and footslope locations. In total, 31 samples were taken from arable land use, 26 from temporary grassland (ley), 14 from permanent grassland and 7 from riparian woodland. Three river-bed sediment samples were collected with a hand trowel and bulked into a single sample on a single occasion at 7 locations along each of the two streams at an (i) upstream (ii) midstream and (iii) downstream location and the joint catchment outlet before the confluence with Loe Pool. Two 0.5 m deep lake sediment cores were taken from Loe Pool c. 150 m below the outlet of Carminowe Creek using a Mackereth corer (Mackereth, 1969).

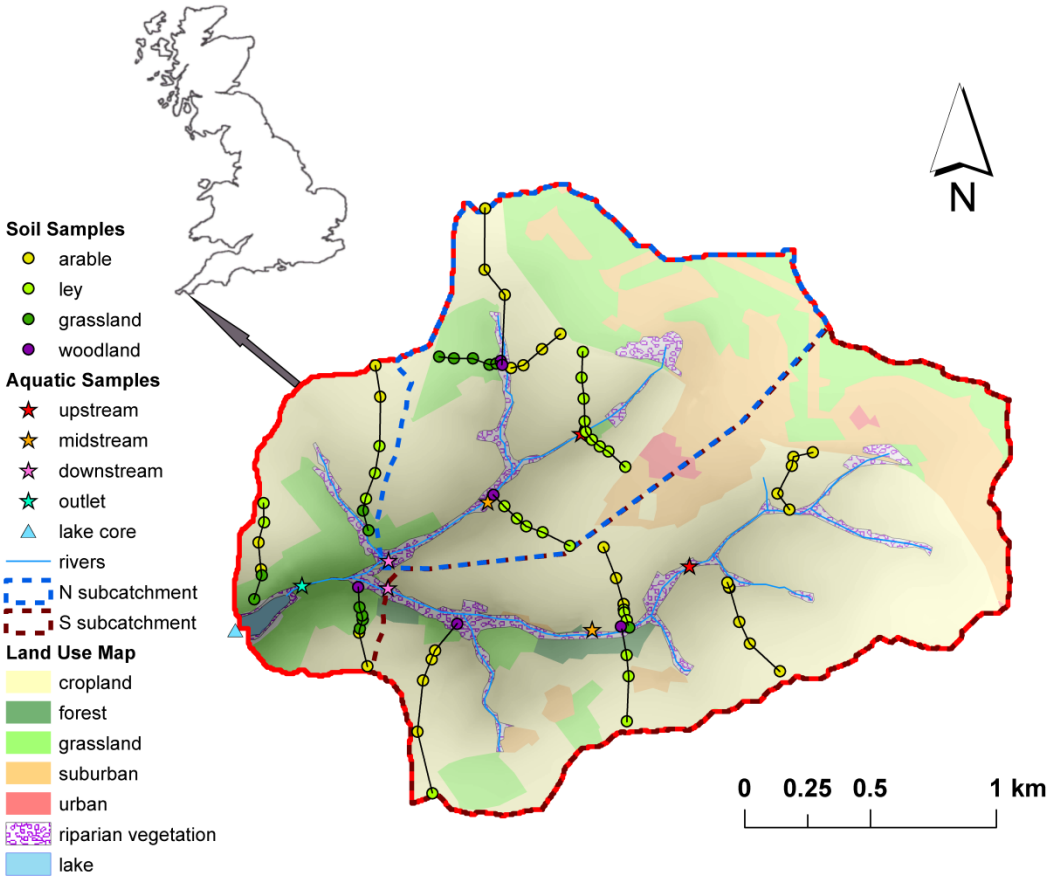

Fig. 1 The study site location in south-west England showing land use, the 14 study transects, river bed sediment sampling locations and the lake core.

2.3 Laboratory analysis

Following sample collection, river bed and lake core sediment samples were stored at 4°C and analysed as soon as possible. Soil samples were oven dried at 40°C and sieved to <2 mm and >2 mm fractions. River bed samples were wet sieved at 250 µm to separate coarse vegetation debris as in Galy et al. (2011) and the < 250 µm fraction was oven dried at 40°C and retained for further analysis. The lake sediment core was sliced into 2 cm increments and freeze dried.

All soil, river bed sediment and lake core samples were analysed for total C, N and bulk $\delta^{13}C$ and $\delta^{15}N$ using a SerCon Integra2 isotope ratio mass spectrometer (SerCon Ltd.,Crewe, UK). An in house standard of Alanine (N=16.7%, C=40%, $\delta^{15}N$=-1.68‰$_{AIR}$, and $\delta^{13}C$=-19.58‰$_{VPDB}$) was used in duplicate every 9 samples to provide quality control and to act as an internal reference. This was calibrated within each analytical run by also analysing International Atomic Energy Agency (IAEA) reference materials N-1 and N-2 for nitrogen and CH-6 and LSVEC for carbon. Due to systematic blanks data had to be blank subtracted and a linearity correction was applied based on the analysis of the IAEA reference materials. The analytical precision of the internal quality control samples of alanine was determined.

The standard deviation of the $\delta^{15}N$ measurements was <0.3‰ and of the $\delta^{13}C$ measurements was <0.1‰. The values were expressed relative to AIR and Vienna PeeDee Belemnite (VPDB) for nitrogen and carbon respectively. The formula used for presenting δ values is as follows:

$$\delta\ ^{15}N\ X\ ‰_{AIR} = (R_{sam}/R_{ref})-1)*1000 \quad (1)$$

$$\delta\ ^{13}C\ X\ ‰_{VPDB} = (R_{sam}/R_{ref})-1)*1000 \quad (2)$$

Where sam is sample and ref is the reference material, R is the ratio of the heavy isotope over the light isotope, X being the isotope ratio expressed in units of per mille (‰).

In order to establish a chronology for the lake core profile, ^{137}Cs assay of individual 2 cm core sections was undertaken at 661.67 KeV using an ORTEC GMX co-axial HPGe γ-detector, coupled to a multi-channel analyser. Sample count times were generally 24 hours, resulting in analytical precision of c. 5%.

On the basis of likely hydrological connectivity with the watercourses we selected a sub-set of 50 samples to estimate *n*-alkane concentrations (μg g^{-1} C) from soil samples Lake core samples were combined into 4 cm increments. . The procedure of total lipid extraction was followed by lipid fractionation to isolate the hydrocarbon fraction for analysis using an Agilent 6890 GC instrument coupled to an Agilent 5973 MS instrument and equipped with an Agilent DB-5 ms column (30 m x 250 μm i.d.x 0.25 μm film thickness). The dominant fragment ions (base peak) were represented by m/z 57 and the diagnostic ions (m/z) 282 (C_{20}), 296 (C_{21}), 324 (C_{23}), 338 (C_{24}), 352 (C_{25}), 366 (C_{26}), 380 (C_{27}), 394 (C_{28}), 408 (C_{29}), 422 (C_{30}), 436 (C_{31}), 450 (C_{32}), 464 (C_{33}) and 478 (C_{34}, internal standard) (Norris, 2013). The concentrations of individual *n*-alkanes were determined relative to the C_{34} internal standard.

Interpretation of *n*-alkane results used the percentage of C_{27}, C_{29} and C_{31} calculated as (Torres et al., 2014):

$$\%\ C_i = C_i/ (C_{27}+C_{29}+C_{31}) \quad (3)$$

where C_i stands for the respective *n*-alkane (C_{27}, C_{29} and C_{31}).

Further, we used the ratio between the shorter chain C_{27} (indicative of woody source (Zech et al., 2009) and longer chain C_{31} (indicative of grass source (Eckmeier and Wiesenberg, 2009) to distinguish between respective contributions of OM from woodland and grassland land uses (Puttock et al., 2014).

2.4 Indicators of aquatic versus terrestrial OM sources

To interpret the relative contribution of higher aquatic vs. terrestrial plants to OM in river and lake sediments we used the following formula (Ficken et al., 2000):

$$PAQ = \frac{(C23+C25)}{(C23+C25+C29+C31)} \quad (4)$$

where PAQ is the ratio of shorter-chain *n*-alkanes (C_{23}+C_{25}) contributed by higher aquatic plants (macrophytes) and mosses to the concentration (in µg g^{-1}) of *n*-alkanes indicative of both aquatic and terrestrial vegetation (C_{23}+C_{25}+C_{29}+C_{31}).

The proportion of OM from terrestrial sources in river bed sediments and in the lake core was calculated using the following formula (Fang et al., 2014; Meyers, 2003)

$$TAR = \frac{(C27+C29+C31)}{(C15+C17+C19)} \quad (5)$$

where TAR is terrestrial/aquatic ratio of the concentration of *n*-alkanes (in µg g^{-1}) derived from terrestrial sources (C_{27}+C_{29}+C_{31}) to those indicative of aquatic algae (C_{15}+C_{17}+C_{19}).

Organic matter degradation in the lake core was examined using the odd-over-even predominance (OEP) *n*-alkane ratio (Zech et al., 2013) as follows:

$$OEP= (nC_{27} + nC_{29} + nC_{31} + nC_{33}) / (nC_{28} + nC_{30} + nC_{32}) \quad (6)$$

High OEPs point either to an increased OM input and/or to an increased OM preservation while low OEPs are indicative of accelerated degradation under aerobic conditions (Zech et al., 2013).

We used $\delta^{13}C$, $\delta^{15}N$ and C/N ratio as further geochemical proxies to understand the proportion of OM contributed by algal *vs.* terrestrial plant derived production as used in previous studies (Fang et al., 2014; Hamilton and Lewis, 1992; Meyers, 2003).

2.5 Statistical Analysis

Kruskal-Wallis non-parametric test was used to examine the differences between elemental (C/N) and isotopic ($\delta^{15}N$, $\delta^{13}C$) signatures between different sediment sources. All soil, river bed sediment and lake core increments were included in this analysis. Principal component analysis (PCA) was used to examine whether elemental and *n*-alkane ratios could be used to distinguish the provenance of sediment sources derived from six potential sources (arable, temporary grassland (ley), permanent grassland, riparian woodland, lake or river bed). All statistical analyses were undertaken in 'R' vs. 3.4.0. Source apportionment was modelled using the Bayesian isotope mixing model of Stable Isotope Analysis in R (SIAR)' (Parnell and Jackson, 2008, R Core Team, 2014).

3. Results & Discussion

3.1 Distinguishing between terrestrial and aquatic organic matter sources

Statistically significant differences ($p<0.001$) in the C/N ratio and bulk stable ^{13}C and ^{15}N isotopic composition of terrestrial soils, river bed sediments and lake core sediments (Table 1), were determined. Woodland and river bed sediments exhibited the highest C/N ratios,

while the lowest C/N ratios were detected in arable and temporary grassland soils. The high C/N ratio in woodland soils and river sediments is characteristic of more recalcitrant OM sources such as wood, while the low C/N ratio is indicative of more decomposable OM with lower lignin content (Brady and Weil, 1999). Percentage C and % N were comparable between the woodland and grassland soils and lake sediments and differed from low % C and % N in cropland soils and river bed sediments, indicating fast OM turnover in cropland rotations and rapid loss of OM and inorganic N from river bed sediments to the downstream lake.

The highest bulk $\delta^{15}N$ values were detected in lake core sediments, followed by grassland and arable soils. Enriched $\delta^{15}N$ values in lake sediments may be due to several processes, including significant macrophyte or riparian-aquatic OM inputs (Fang et al., 2014), increased denitrification in anoxic lake bottom waters, and increased net primary production (Meyers, 2003). Increased bulk $\delta^{15}N$ values on arable land may be indicative of both rapid turnover of OM and long-term application of manure (Glendell et al., 2014b). Bulk $\delta^{13}C$ values were relatively uniform between land uses, reflecting the predominance of C3 plants in the study catchment (Puttock et al., 2014). $\delta^{13}C$ values were enriched in arable soils and lake core sediments, with the former possibly reflecting periodic growing of maize, a C4 plant with a different photosynthetic pathway with natural abundance $\delta^{13}C$ values of ~-12‰ (Beniston et al., 2015; Puttock et al., 2014) on arable land and the effect of in-lake organic matter production on lake bed sediments (Fang et al., 2014; Hamilton and Lewis, 1992). However, it is important to acknowledge that direct characterisation of the composition of autochthonous OM produced by aquatic plants in the lake ecosystem would allow a more conclusive interpretation of these findings.

Table 1 Elemental and isotopic composition (mean and SD in brackets) of all terrestrial soils, river bed sediment and lake core samples. Values followed by the same letter are not significantly different, while values followed by a different letter are significantly different ($p<0.05$). N = number of replicates.

Landuse (N)	C/N	$\delta^{15}N$ (‰)	$\delta^{13}C$ (‰)	% C	% N
Arable (31)	8.99 (0.7) a	5.5 (0.8) a	-27.6 (0.4) a	2.92 (0.54)a	0.32 (0.05)a
Grass (14)	9.98 (0.8) b	5.6 (1.2) a, c	-28.2 (0.5) b	5.60 (1.21)b	0.56 (0.14)b
Ley (26)	9.23 (0.7) a	5.5 (0.9) a, c	-28.2 (0.40) b	3.60 (0.82)c	0.39 (0.07)c
Woodland (7)	12.84 (2.4) c	4.7 (1.5) a, c	-28.2 (0.3) b	8.06 (1.83)b	0.63 (0.14)bd
River (7)	12.20 (1.0) c	4.5 (1.1) a, d	-28.3 (0.2) b	2.34 (0.84)a	0.19 (0.06)a
Lake (27)	10.76 (0.6) c	6.3 (0.4) b	-27.6 (0.4) a	7.40 (1.08)b	0.69 (0.07)d

Concentrations of *n*-alkanes of chain lengths C_{15}-C_{33} in the six environments of interest showed a higher concentration of woody- (C_{27}-C_{29}) and grass- (C_{31}) derived OM input in lake sediments, as compared to terrestrial soils. Concurrently, shorter-chain *n*-alkanes indicative of aquatic macrophytes and lower plants such as mosses (C_{21}-C_{25}) (Meyers, 2003) were also apparent in lake sediments and in riparian woodland (Table 2). As expected, C_{31} chain lengths indicative of grasses (forage and cereals) (Eckmeier and Wiesenberg, 2009), were

more abundant in the soils of arable, temporary ley and permanent grassland land uses, while the C_{27} chain-length *n*-alkanes, indicative of woody vegetation (Zech et al., 2009), were more abundant in woodland soils, river bed and lake core sediments.

Table 2 *n*-alkane concentrations (µg g-1 C) in soils and sediments from the six target environments. N – number of replicates.

N	n-alkane chain length concentration µg g^{-1} C Mean (SD)									
Landuse	C15	C17	C19	C21	C23	C25	C27	C29	C31	C33
Arable (11)	0.16 (0.11)	0.22 (0.12)	n/a	0.65 (0.73)	0.22 (0.11)	0.40 (0.12)	0.93 (0.34)	2.68 (1.27)	3.86 (0.91)	1.99 (0.48)
Grass (7)	0.26 (0.18)	0.26 (0.17)	n/a	0.43 (0.17)	0.35 (0.20)	0.76 (0.33)	1.86 (1.32)	3.81 (1.32)	5.52 (1.25)	3.02 (1.02)
Ley (9)	0.25 (0.25)	0.32 (0.29)	n/a	0.92 (0.98)	0.46 (0.70)	0.83 (0.79)	1.29 (0.74)	3.10 (1.09)	4.79 (1.46)	2.22 (0.91)
Woodland (4)	0.11 (0.13)	0.22 (0.24)	n/a	0.94 (0.86)	0.92 (0.69)	2.98 (1.09)	12.93 (6.29)	13.89 (5.09)	7.40 (2.86)	4.40 (2.61)
River (7)	0.24 (0.20)	0.24 (0.21)	0.22 (0.09)	0.46 (0.40)	0.37 (0.20)	1.35 (0.51)	5.70 (2.11)	5.92 (2.24)	2.65 (1.04)	1.10 (0.52)
Lake (12)	0.26 (0.18)	1.28 (0.85)	0.96 (0.42)	0.96 (0.43)	1.90 (0.70)	4.17 (1.42)	16.45 (4.27)	16.62 (2.91)	12.08 (1.55)	4.93 (1.23)

Relative contribution of aquatic *vs.* terrestrial plants to OM was assessed with three indicators, C_{27}/C_{31} ratios, PAQ and TAR. As expected highest C_{27}/C_{31} ratios, indicative of woody sources were found in the woodland soil samples, while low C_{27}/C_{31} ratios in the remaining terrestrial soils were indicative of OM origin from grassland vegetation (including cereal crops and forage grass). The river bed sediments were also characterised by higher C_{27}/C_{31} ratios, indicating predominant sediment input from soils under woody vegetation in the well-connected wooded riparian buffer strip (Fig. 2a). The lake sediments appear to be intermediary between these land uses, indicating OM contribution from both woody and grass vegetation, which may be related to OM transport during high-flow events. During rainfall events, the less connected arable/grassland sources may make a greater contribution to OM transport, which is likely to be directly routed to the lake, without being deposited in river bed sediments.

Higher median PAQ ratios of > 0.15 in the lake, river and riparian woodland environments were indicative of emergent macrophyte origin, while the lower median ratios <0.1 were indicative of terrestrial plants (Fig. 2b). The higher PAQ ratios in the riparian woodland may reflect a contribution from lower plants including mosses, which were abundant on the ground of this wet woodland. Still there remains a large unexplained variability of observed PAQ, particularly in the grass ley.

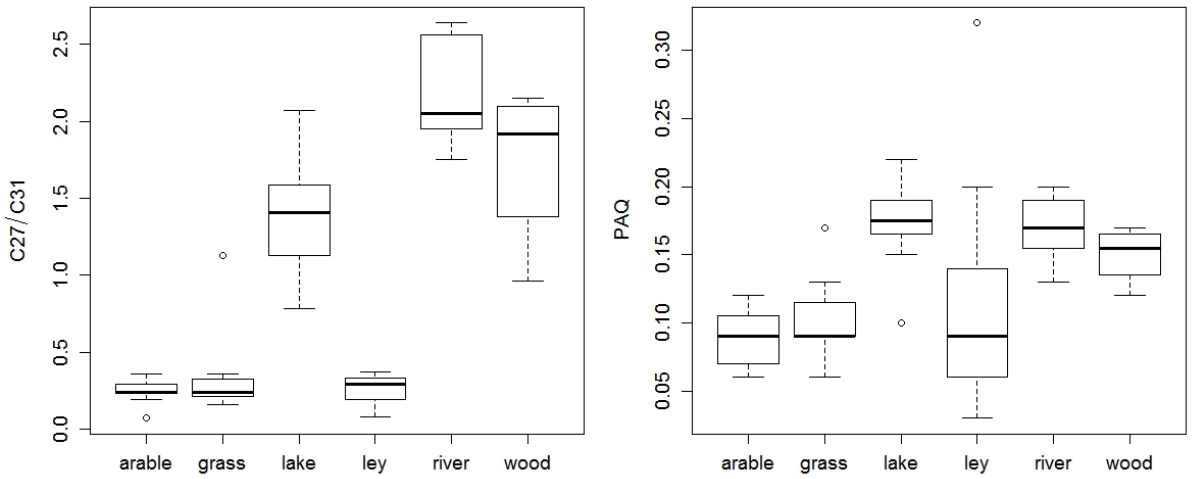

Fig. 2 Box plots of *n*-alkane ratios a) C_{27}/C_{31} indicating OM prevalence from woody *vs*. grass dominated sources b) PAQ indicating contribution of OM from aquatic/lower plant *vs*. terrestrial vegetation. The bottom and top of the box refer to the 25th and 75th percentile, the bold line near the middle to the 50th percentile (the median) and whiskers following the default setting of R, respectively.

While single tracers and ratios presented above cannot unravel contribution of several sources on their own, a global assessment with a Principal Component Analysis (PCA) was undertaken. PCA revealed that a combined *n*-alkane, elemental and stable ^{13}C and ^{15}N isotopic signatures provide a clear separation in sediment fingerprint composition (Fig. 3). The PCA axis 1 can be interpreted as a gradient between grassland and arable land uses with higher % C_{31} *n*-alkane signature (indicating grass-derived OM) *vs*. riparian woodland and aquatic environments with a higher % $C_{27,}$ higher C_{27}:C_{31} and C/N ratios (indicating wood-derived OM sources), lower % C_{29} (indicating lower plants in the woodland ground vegetation) and higher PAQ (Tables 2-4, Fig. 3a). The PCA axis 2 can be interpreted as a gradient between river bed sediments and lake core sediments, with the latter supporting higher $\delta^{13}C$ and $\delta^{15}N$ isotopic signatures and higher % C and % N content (Tables 2-4, Fig. 3a) and indicating different sediment dynamics in the two aquatic environments. This is also reflected in Fig 3b, which shows a clear distinction in sediment composition between lake and river bed sediments and woodland, permanent grassland and cropland sources. However, PCA could not distinguish soils from temporary grassland (ley) and arable land, presumably because these two land uses are subject to regular rotations. While other researchers have also found it possible to distinguish between permanent grassland and woodland sediment and OM sources, they were unable to distinguish between arable land use and permanent grassland, based on the use of biomarkers alone (Alewell et al., 2015). In this study, the combined use of biomarkers and elements (% C, % N, C/N ratio) allowed us to distinguish between these two land uses as the % N and % C as well as C/N ratio are all higher in grassland soils than in arable and temporary grass ley (Tables 3-4), thus acting as further informative tracers in addition to *n*-alkanes.

356 Table 3 Biogeochemical values (mean and SD) of the 50 source soils, river bed sediments
357 and lake core samples included in the PCA analysis. N = number of replicates.

Land use (N)	C_{27}:C_{31}	PAQ	% C_{27}	% C_{29}	% C_{31}	% N	$\delta^{15}N$ (‰)	% C	C/N	$\delta^{13}C$ (‰)
	Mean (SD)									
Arable (11)	0.25 (0.08)	0.09 (0.02)	0.13 (0.04)	0.35 (0.06)	0.52 (0.06)	0.33 (0.05)	5.3 (1.03)	3.05 (0.64)	9.32 (0.97)	-27.6 (0.42)
Grass (7)	0.37 (0.34)	0.10 (0.04)	0.16 (0.07)	0.33 (0.04)	0.51 (0.11)	0.52 (0.10)	5.2 (1.21)	5.40 (1.08)	10.39 (0.86)	-28.0 (0.57)
Ley (9)	0.26 (0.10)	0.12 (0.09)	0.13 (0.04)	0.34 (0.01)	0.53 (0.04)	0.40 (0.08)	5.2 (0.63)	3.77 (1.07)	9.21 (0.86)	-28.2 (0.33)
Woodland (4)	1.74 (0.54)	0.15 (0.02)	0.37 (0.07)	0.41 (0.05)	0.22 (0.04)	0.62 (0.16)	4.7 (1.97)	7.80 (2.29)	12.67 (3.23)	-28.3 (0.31)
River (7)	2.21 (0.37)	0.17 (0.03)	0.40 (0.03)	0.41 (0.02)	0.19 (0.02)	0.19 (0.06)	4.5 (1.06)	2.34 (0.84)	12.20 (1.01)	-28.3 (0.24)
Lake (12)	1.37 (0.37)	0.17 (0.03)	0.36 (0.05)	0.37 (0.01)	0.27 (0.05)	0.70 (0.07)	6.4 (0.31)	7.61 (0.95)	10.91 (0.46)	-27.7 (0.41)

358

359 Table 4 Loading scores of ten biochemical tracers, initial eigenvalues and % total variance
360 accounted for by the first three PCA axes with eigenvalues >1. Loading scores >0.3 were
361 used in the interpretation of axes.

	axis 1	axis 2	axis 3
%N	0.33	0.86	-0.34
delta 15N		0.74	0.48
%C	0.49	0.75	-0.45
C/N	0.74		-0.38
delta 13C		0.49	0.34
C27/C31	0.92		
PAQ	0.66		0.35
C27	0.95		
C29	0.63	-0.46	

C31	-0.97		
Arable	-2.17	-0.40	
Grass	-1.22	0.42	-0.81
Lake	1.71	1.80	
Ley	-1.77		
River	2.39	-2.48	0.91
woodland	2.79		-1.28
Eigenvalues	4.49	2.38	1.06
% of variance	44.90	23.82	10.65
Cumulative % of variance	44.90	68.71	79.36

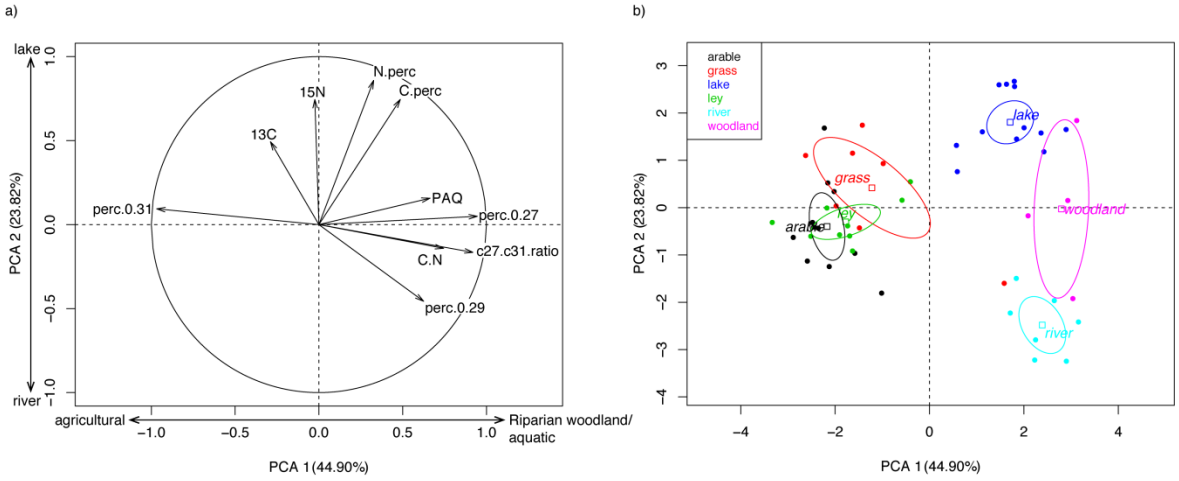

Fig. 3 Two-dimensional plot of a) variable distribution along the first two PCA ordination axes b) sampling site loading scores on the first two PCA axes and 95% confidence ellipses around the categories of land use.

3.2 Spatial variability of land use and provenance of OM in river bed sediments

Spatial patterns of OM provenance in relation to land use were examined at each river bed sediment sampling location ("upstream", midstream", "downstream" and "outlet") in the two subcatchments (S and N) (Figs. 1, 4, 5). Organic matter fingerprinting properties reflected some subtle differences in land used between the two subcatchments. While both the S and N subcatchments were characterized by ca. 75 % agricultural land use, 20 % sub-urban land

373 use and 5 % of riparian vegetation in the riparian corridor, the S subcatchment supported a
374 higher arable and ley *vs*. permanent grassland ratio (65 % to 10 %, respectively) than the N
375 subcatchment (48 % to 19 %, respectively) (Fig. 4).

376

377

378 Fig. 4 Proportion of different land uses a) at the outlet sampling location b) the whole study
379 catchment c) Southern subcatchment and d) Northern subcatchment.

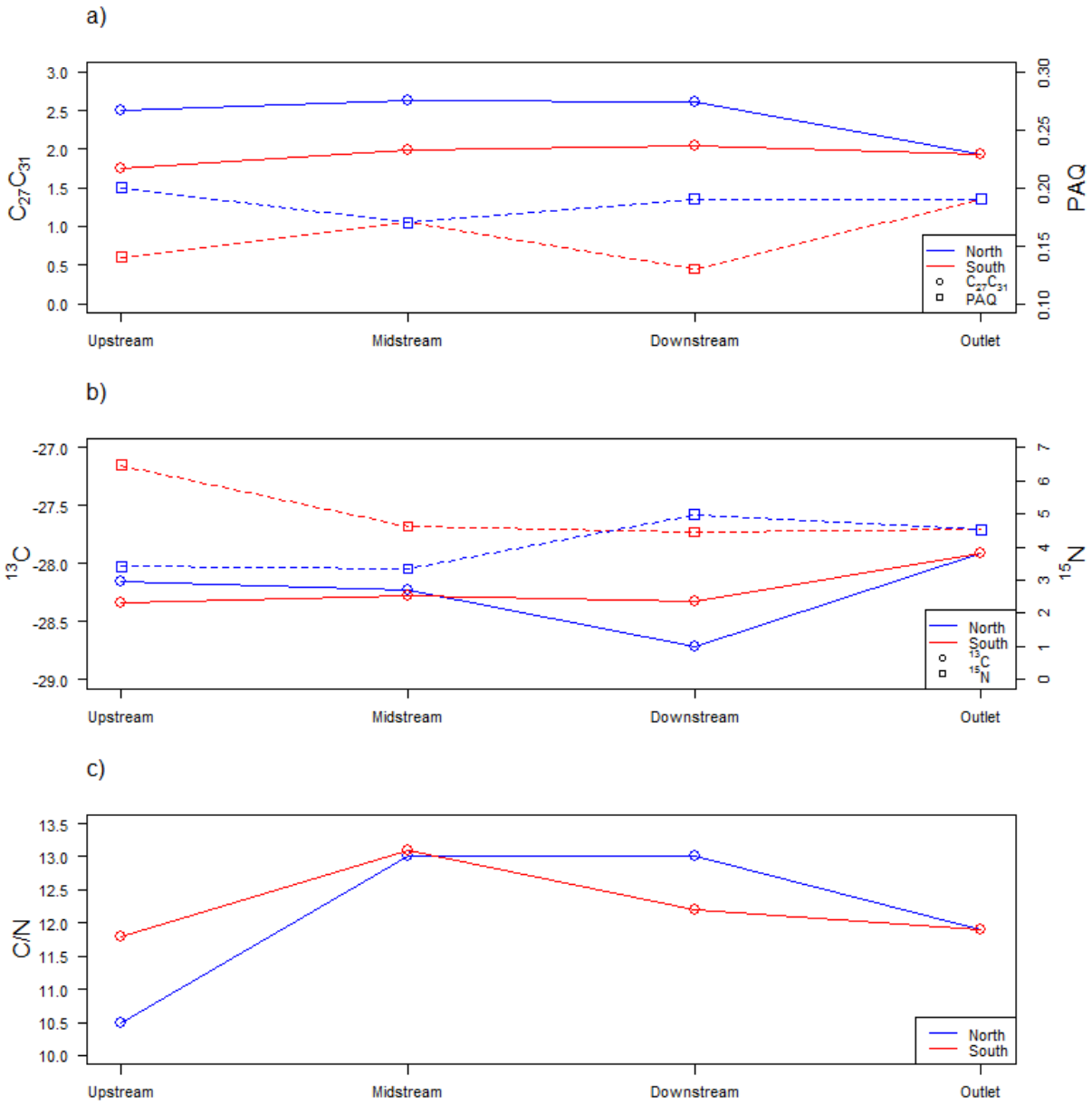

Fig. 5 Spatial variability of a) *n*-alkane proxies b) stable isotopes and c) C/N ratio in a downstream direction in the two subcatchments.

This was reflected in river bed OM properties, which had lower C_{27}/C_{31} ratios than in the N subcatchment, with the upstream location supporting the lowest C_{27}/C_{31} *n*-alkane value of 1.75 overall (Fig 5a), likely due to a higher proportion of arable and ley land use in this subcatchment (Fig 4c) leading to higher soil erosion rates (Turnage et al., 1997). The observed higher $\delta^{15}N$ values at the most upstream location (ca.+7 ‰, Fig 5b) may also be associated with a higher application of farmyard manure and slurry to arable land and ley (Bol et al., 2005; Senbayram et al., 2008). Conversely, the higher C_{27}/C_{31} ratio in the N subcatchment and the lack of upstream forested areas indicate a higher contribution of OM from wooded vegetation in the riparian zone, as well as a potential buffering of terrestrial OM fluxes from agricultural soils in the vegetated river corridor. Higher PAQ ratios in the N subcatchment, indicating a relatively higher contribution of mosses and macrophytes derived

OM, also point towards a greater influence of the riparian zone on lateral C fluxes as compared to the S stream (Fig. 5a).

Higher C_{27}/C_{31} and C/N ratios (Fig. 5a & 5c) at the midstream and downstream locations in both subcatchments indicated an increased contribution of OM from woody vegetation to river bed sediments in these river reaches. The C_{27}/C_{31} *n*-alkane ratio at the joint catchment outlet was lower than in the N subcatchment but similar to the ratios found in the S sub-catchment (Fig. 5a), indicating mixing of OM from the two tributaries as well as input from permanent grasslands situated on the steep slopes in the lower reaches of the river corridor.

3.3 Impact of land use on sediment and C accumulation in lake bed sediments

Source apportionment modelling of the lake core sediments has shown different results, depending on the composition of the fingerprint signatures. Currently, there is a lack of consensus within the sediment fingerprinting community on the most appropriate selection of fingerprint tracers (Sherriff et al., 2015; Zhang and Liu, 2016). Therefore, in this study, we firstly included all tracers used in the PCA in the source apportionment analysis (Fig. 6a), followed by just those tracers that encompassed the range of values represented in the mixture (and therefore deemed as conservative) (Fig. 6b). The second approach included C_{27}:C_{31} ratio, % C_{27}, % C_{29} and % C_{31}. As such we had 4 tracers (n) to apportion the contribution of five sources (n+1). In both cases, organic C from riparian woodland was a major contributor to the lake sediments. In the second scenario, river bed sediments appeared to make the second largest contribution to lake core sediments over the past 60 years (Fig. 6b). However, as river bed sediments are also dominated by woody vegetation, as shown in Fig. 2a above, they can be considered ‘equal to’ woodland signatures in this apportionment model, due to the restricted number of very selective tracers. However, in both modelling outcomes, the important contribution of organic matter from permanent grassland, which occupies the steep slopes surrounding the lake, is very apparent (Fig. 6a).

Zhang and Liu (2016) also found that tracer selection greatly impacted the estimated source contributions, due to a number of potential reasons, including i) tracer conflicts ii) tracer measurement error and iii) differences in tracer conservativeness. Therefore, they proposed to use multiple fingerprints to derive ‘average’ estimated source contribution proportions, instead of just a single fingerprint set. While different sediment contributions can be obtained with different fingerprint selection, recent studies (Palazón et al., 2015; Sherriff et al., 2015) have found that inclusion of more tracers improved the source apportionment results. In this study, modelling results based on the full set of tracers (Fig. 6a) allowed a finer distinction between contributing land uses.

Conversely to lake core sediments, it was not possible to model the source apportionment of river bed sediments satisfactorily as all potential tracers in bed sediments appeared to be outside the range of the potential sources. This apparently 'missing source' opens new lines of enquiry for future research. At present we hypothesise that the 'missing source' may either be due to the contribution of petrogenic C originating from the underlying bedrock (Galy et al., 2015) or that the *n*-alkane signatures have been altered by autochtonous in-stream production of OM (e.g. from algae) and by in-stream biological processing of river bed sediments (Chen et al., 2016).

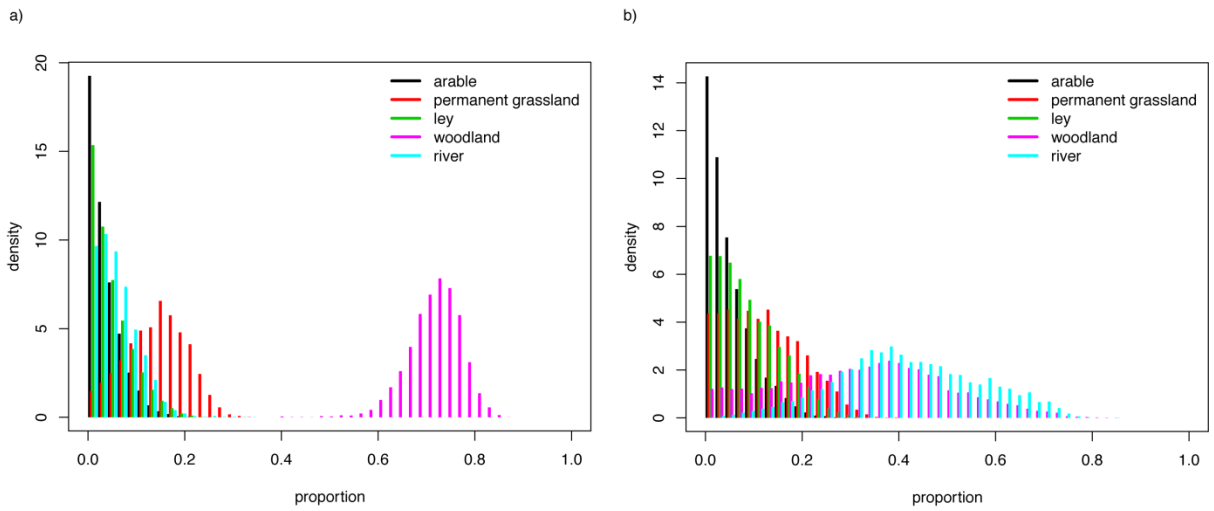

Fig. 6 Probability density function of sediment source apportionment sources from different land uses using a) all available tracers b) only tracers that encompass the full range of values present in the mixture for the application of the mixing model SIAR.

3.4 Understanding the temporal variability of lateral C fluxes from land to water in relation to land use change

Caesium-137 (^{137}Cs) activity was used to get an approximate dating profile for the lake bed sediment core (Fig. 7a). The depth distribution of ^{137}Cs within the core was analysed and the horizon containing peak activity was identified at 26 cm and was assumed to be associated with the peak in bomb derived ^{137}Cs fallout attributed to 1963. The offset of bomb testing in 1952 was assumed to be associated with lake core depth at 34 cm.

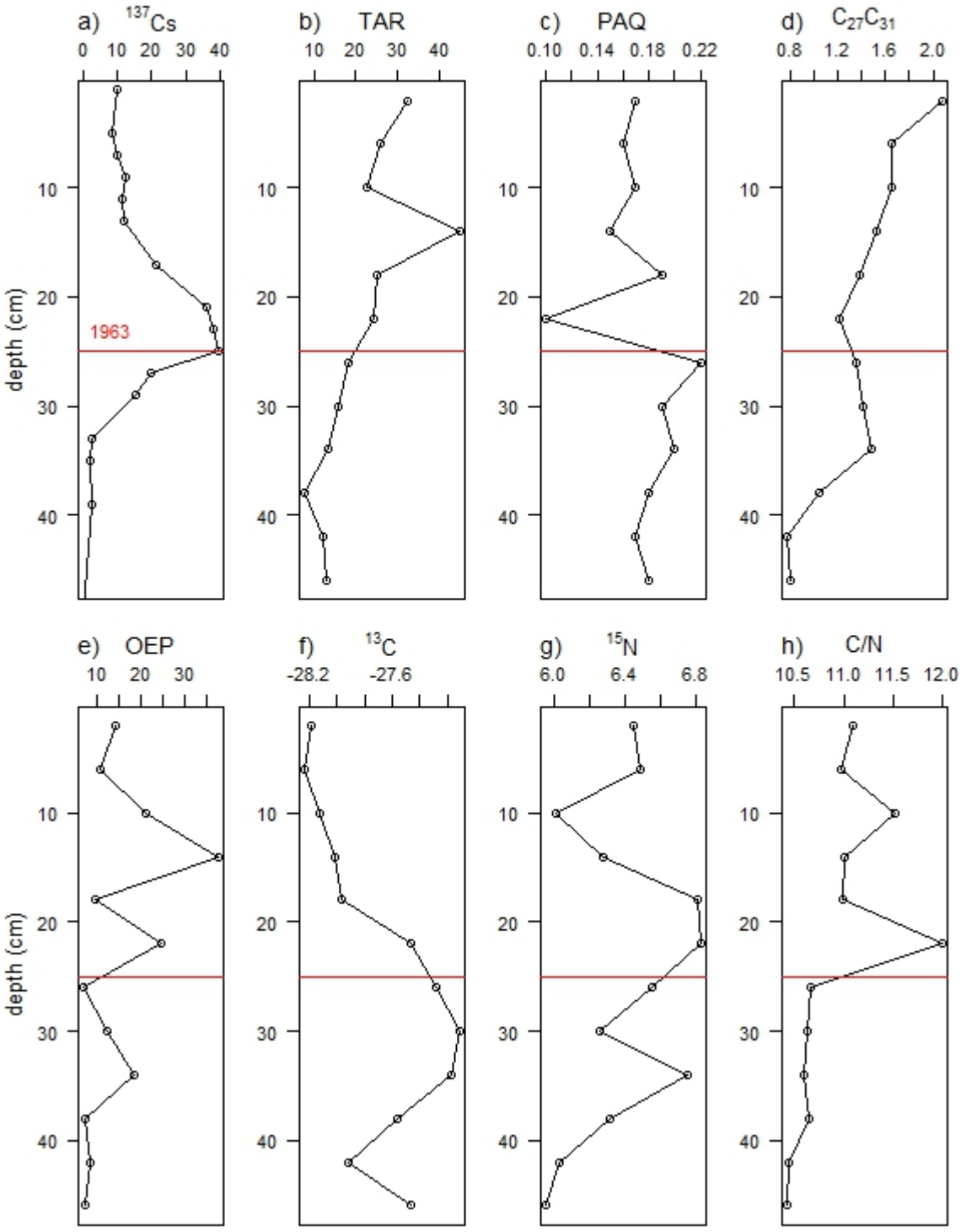

Figure 7 Lake core profiles showing a)^{137}Cs activity used to date the lake sediment core and interpret the observed changes in sediment composition over time b-h) sediment fingerprinting characteristics with depth.

The combined use of *n*-alkane ratios and stable isotope signatures shows a variable contribution of terrestrial *vs*. aquatic sources to sediment accumulation in individual lake core increments over the past 60 years (Fig. 7b-h). The TAR ratio (Fig. 7b) indicates an increasing contribution of terrestrial-derived OM to the lake sediments, while the increasing C_{27}/C_{31} ratio (Fig. 7d) indicates an increase of woody vegetation contribution over the same time period. This is corroborated by the fact that the signal from PAQ *n*-alkane proxy lies within the range of 0.01 to 0.23 (Fig. 7c), deemed indicative of terrestrial plants (Silliman and Schelske, 2003) and suggesting mainly allochthonous source of sedimentary OM. The depletion in $\delta^{13}C$ values with depth (Fig. 7f) may also indicate an increasing input of isotopically lighter soil-derived dissolved inorganic C (Meyers, 2003) – and thus increasing terrestrial input of C from soil erosion. However, it may also be due to the preferential loss of the light isotope (^{12}C) through microbial respiration over time (Beniston, et al. 2014). In any case correlation between OEP and TAR ratios ($p<0.001$, $R^2=0.53$) suggests reduced OM decomposition associated with increasing terrestrial contribution of OM over the past 60 years (Zech et al., 2013), which may be linked to a higher C/N ratio – and therefore lower bioavailability of woodland and grassland derived OM.

While increased $\delta^{15}N$ enrichment (Fig. 7g) may be indicative of increased net primary production associated with the reported eutrophication of Loe Pool since the 1960s (Dinsdale, 2009), it is not likely to be due to an increase in N fixing cyanobacteria, which directly fix atmospheric N_2 and therefore lead to lower $\delta^{15}N$ signatures in sediments and would be expected to lead to an increased $\delta^{13}C$ signature due to enhanced NPP (Meyers and Lallier-Vergès, 1999; Meyers, 2003). In addition, increased $\delta^{15}N$ enrichment may be associated with enhanced denitrification (preferential loss of the light ^{14}N isotope) in anoxic lake bottom waters (Meyers, 2003) or with higher natural abundance ^{15}N-enriched signatures originating from faeces from farmyard manures (Senbayram et al. 2008) and septic tanks (Collins, et al. 2013; 2014).

However, it is acknowledged that $\delta^{13}C$ enrichment and C/N ratios are not always indicative of sources as they can be affected by degradation (Ranjan et al., 2015). Laceby et al. (2015) found that while $\delta^{15}N$ bulk isotopic signatures of sediment sources exhibited non-conservative behaviour, $\delta^{13}C$ signatures appeared to be more stable. Fang et al. (2014) observed that significant macrophyte or riparian-aquatic OM inputs may lead to higher $\delta^{15}N$ and $\delta^{13}C$ values in lake sediments, thus confounding our ability to distinguish between the terrestrial and aquatic input of OM on the basis of bulk stable ^{13}C and ^{15}N isotopic signatures alone. Therefore, compound-specific stable ^{13}C isotope (CSSIA) signatures of plant-derived biomarkers are currently explored as more suitable tracers, as the isotopic signatures of individual molecules are likely to be more conservative than bulk stable isotopes alone (Fang et al., 2014; Tao et al., 2016).

In this study, the combined use of *n*-alkanes and bulk stable ^{13}C and ^{15}N isotopes detected increased terrestrial input of sediment and increased lake eutrophication over the past 60 years, with terrestrial grass and woody plant-derived *n*-alkanes being more indicative of OM sources, and stable ^{13}C and ^{15}N isotopes being more indicative of in-stream and in-lake

processes. The application of compound-specific stable isotope $\delta^{13}C$ and $\delta^{2}H$ signatures of specific *n*-alkane molecules, as opposed to a separate use of *n*-alkane chain length and bulk stable ^{13}C and ^{15}N isotopes, may help to better differential between aquatic and terrestrial plant origin of organic matter in future work (Cooper et al., 2015) and thus quantify the autochtonous *vs*. allochtonous organic matter contribution. Further improvements may be obtained by multi-molecular investigations using simultaneous application of different biomarkers and ^{14}C isotopes to constrain the transfer of C from land to the ocean (Feng et al., 2015).

The ability to discern OM contribution to aquatic environments from different land uses found in this study, provides an important new tool for the understanding of OM fluxes from land to water at catchment scales. Wohl et al. (2017) proposed a revised paradigm for the understanding of the role of rivers in the transport and processing of terrestrial C, whereby the active river channel and the riparian zone function as one coupled system – a *river corridor*, in which riparian areas act 'as biogeochemical reactors that facilitate the speciation, transformation, and opportunities for both long-term storage of carbon and mineralization to the atmosphere'. Wohl et al. (2017) posit that while alteration of riparian zone is the most significant and most highly altered aspect of lateral C dynamics, very little is known about the sources and quantities of different kinds of OM stored within river corridors and how C inputs have varied over decadal and millennial timescales as a results of human activities. In this study, we also found very close coupling between the aquatic sediments and the riparian zone and our ability to discern between these sources provides a new opportunity to quantify the lateral C fluxes at catchment scales. Coupling the fingerprinting approach explored in this paper with future modelling of soil erosion rates is a promising new tool for quantifying these lateral C fluxes at a range of scales.

4. Conclusions

This pilot study tested a new approach to quantify the lateral fluxes of OM from the terrestrial to aquatic environments at a catchment scale. Here we evaluated the combined use of the abundance and ratios of conservative plant-derived biomarkers *n*-alkanes and bulk stable isotopes to distinguish between OM and sediment provenance from different environments. While it was possible to distinguish between arable and temporary grassland, permanent grassland, woodland, river and lake environments, it was not possible to distinguish between arable land and temporary grassland, as these two land uses are part of regular rotations. However, the combined use of biomarkers and stable isotopes allowed us to distinguish between sediment sources from arable and permanent grassland land uses, which has not been previously possible with the use of biomarkers alone. Furthermore, the combined use of biomarkers and stable isotopes enabled us to detect the observed change in the lake trophic status over the past 60 years and attribute this to changing land use, resulting in enhanced sedimentation and nutrient flux from the terrestrial to the aquatic environments. These enhanced lateral OM fluxes can be linked to agricultural intensification, resulting in higher soil erosion rates, over the same period. Moreover, we detected an increased contribution of

104 woody vegetation to the OM provenance over time, most likely indicating an increase in the
105 woody vegetation covering the near-stream riparian corridor. The new fingerprinting
106 approach successfully discriminated between terrestrial *vs*. aquatic C sources and when
107 coupled with quantitative estimates of soil erosion rates, it shows to be a promising new tool
108 for the understanding of lateral C fluxes from land to water at a range of scales. The close
109 coupling between OM provenance and riparian land use observed in this study underlines the
110 importance of the riparian zone for lateral C transfers and thus support the new holistic
111 conceptualization of 'river corridors' as critical zones linking the terrestrial and aquatic C
112 (Wohl et al., 2017).

113

114 **Acknowledgements** This work was supported by the University of Exeter Strategic Science
115 Development Fund and UK Natural Environment Research Council GW4+ Research
116 Experience Placement Scheme. We would like to thank Iain Hartley and Gabriel Yvon-
117 Durocher of the University of Exeter for helpful scientific discussions at the project inception
118 and to two anonymous reviewers for their constructive comments that greatly helped to
119 improve our manuscript

120

121 **References**

122 Adhikari, K., Hartemink, A.E., 2016. Linking soils to ecosystem services - A global review.
123 Geoderma 262, 101–111. doi:10.1016/j.geoderma.2015.08.009

124 Alewell, C., Egli, M., Meusburger, K., 2015. An attempt to estimate tolerable soil erosion
125 rates by matching soil formation with denudation in Alpine grasslands. J. Soils
126 Sediments 1–17. doi:10.1007/s11368-014-0920-6

127 Alewell, C., Birkholz, A., Meusburger, K., Schindler Wildhaber, Y., Mabit, L., 2016.
128 Quantitative sediment source attribution with compound-specific isotope analysis in a
129 C3 plant-dominated catchment (central Switzerland). Biogeosciences 13, 1587–1596.
130 doi:10.5194/bg-13-1587-2016

131 Alewell, C., Birkholz, A., Meusburger, K., Schindler Wildhaber, Y., Mabit, L., 2015.
132 Sediment source attribution from multiple land use systems with CSIA. Biogeosciences
133 Discuss. 12, 14245–14269. doi:10.5194/bgd-12-14245-2015

134 Amundson, R., Berhe, A.A., Hopmans, J.W., Olson, C., Sztein, A.E., Sparks, D.L., 2015.
135 Soil science. Soil and human security in the 21st century. Science 348, 1261071.
136 doi:10.1126/science.1261071

137 Aufdenkampe, A.K., Mayorga, E., Raymond, P.A., Melack, J.M., Doney, S.C., Alin, S.R.,
138 Aalto, R.E., Yoo, K., 2011. Riverine coupling of biogeochemical cycles between land,
139 oceans, and atmosphere. Front. Ecol. Environ. 9, 53–60. doi:10.1890/100014

140 Battin, T.J., Luyssaert, S., Kaplan, L. a., Aufdenkampe, A.K., Richter, A., Tranvik, L.J.,
141 2009. The boundless carbon cycle. Nat. Geosci. 2, 598–600. doi:10.1038/ngeo618

142 Beniston, J.W., DuPont, S.T., Glover, J.D., Lal, R., Dungait, J.A.J., 2014. Soil organic carbon

dynamics 75 years after land-use change in perennial grassland and annual wheat agricultural systems. Biogeochemistry 120, 37–49.

Beniston, J.W., Shipitalo, M.J., Lal, R., Dayton, E.A., Hopkins, D.W., Jones, F., Joynes, A., Dungait, J.A.J., 2015. Carbon and macronutrient losses during accelerated erosion under different tillage and residue management. Eur. J. Soil Sci. 66, 218–225.

Bilotta, G.S., Brazier, R.E., 2008. Understanding the influence of suspended solids on water quality and aquatic biota. Water Res. 42, 2849–2861. doi:10.1016/j.watres.2008.03.018

Blake, W.H., Ficken, K.J., Taylor, P., Russell, M.A., Walling, D.E., 2012. Tracing crop-specific sediment sources in agricultural catchments. Geomorphology 139–140, 322–329. doi:10.1016/j.geomorph.2011.10.036

Bol, R., Eriksen, J., Smith, P., Garnett, M.H., Coleman, K., Christensen, B.T., 2005. The natural abundance of 13C, 15N, 34S and 14C in archived (1923-2000) plant and soil samples from the Askov long-term experiments on animal manure and mineral fertilizer. Rapid Commun. Mass Spectrom. 19, 3216–3226.

Brady, N.C., Weil, R.R., 1999. The Nature and Properties of Soils. Prentice Hall, Upper Saddle River, New Jersey.

Brevik, E.C., Cerdà, a., Mataix-Solera, J., Pereg, L., Quinton, J.N., Six, J., Van Oost, K., 2015. The interdisciplinary nature of *SOIL*. Soil 1, 117–129. doi:10.5194/soil-1-117-2015

Chen, F., Fang, N., Shi, Z., 2016. Using biomarkers as fingerprint properties to identify sediment sources in a small catchment. Sci. Total Environ. 557–558, 123–133. doi:10.1016/j.scitotenv.2016.03.028

Chen, F.X., Fang, N.F., Wang, Y.X., Tong, L.S., Shi, Z.H., 2017. Biomarkers in sedimentary sequences: Indicators to track sediment sources over decadal timescales. Geomorphology 278, 1–11. doi:10.1016/j.geomorph.2016.10.027

Cole, J.J., Prairie, Y.T., Caraco, N.F., McDowell, W.H., Tranvik, L.J., Striegl, R.G., Duarte, C.M., Kortelainen, P., Downing, J.A., Middelburg, J.J., Melack, J., 2007. Plumbing the global carbon cycle: Integrating inland waters into the terrestrial carbon budget. Ecosystems 10, 171–184. doi:10.1007/s10021-006-9013-8

Collins, A.L., Williams, L.J., Zhang, Y.S., Marius, M., Dungait, J.A.J., Smallman, D.J., Dixon, E.R., Stringfellow, A., Sear, D.A., Jones, J.I., Naden, P.S., 2013. Catchment source contributions to the sediment-bound organic matter degrading salmonid spawning gravels in a lowland river, southern England. Sci. Total Environ. 456, 181–195.

Collins, A.L., Williams, L.J., Zhang, Y.S., Marius, M., Dungait, J.A.J., Smallman, D.J., Dixon, E.R., Stringfellow, A., Sear, D.A., Jones, J.I., Naden, P.S., Collins, A.L., Williams, L.J., Zhang, Y.S., Marius, M., Dungait, J.A.J., Smallman, D.J., Dixon, E.R., Stringfellow, A., Sear, D.A., Jones, J.I., Naden, P.S., 2014. Sources of sediment-bound organic matter infiltrating spawning gravels during the incubation and emergence life stages of salmonids. Agric. Ecosyst. Environ. 196, 76–93. doi:10.1016/j.agee.2014.06.018

Cooper, R.J., Pedentchouk, N., Hiscock, K.M., Disdle, P., Krueger, T., Rawlins, B.G., 2015. Apportioning sources of organic matter in streambed sediments: An integrated molecular and compound-specific stable isotope approach. Sci. Total Environ. 520, 187–197. doi:10.1016/j.scitotenv.2015.03.058

Dinsdale, J., 2009. Loe Pool Catchment Management Project 2009 Review.

Eckmeier, E., Wiesenberg, G.L.B., 2009. Short-chain n-alkanes (C16-20) in ancient soil are useful molecular markers for prehistoric biomass burning. J. Archaeol. Sci. 36, 1590–1596. doi:10.1016/j.jas.2009.03.021

Eglinton, G., Gonzalez, A.G., Hamilton, R.J., Raphael, R.A., 1962. Hydrocarbon constituents of the wax coatings of plant leaves: A taxonomic survey. Phytochemistry 1, 89–102.

Fang, J., Wu, F., Xiong, Y., Li, F., Du, X., An, D., Wang, L., 2014. Source characterization of sedimentary organic matter using molecular and stable carbon isotopic composition of n-alkanes and fatty acids in sediment core from Lake Dianchi, China. Sci. Total Environ. 473–474, 410–21. doi:10.1016/j.scitotenv.2013.10.066

Feng, X., Gustafsson, Holmes, R.M., Vonk, J.E., Van Dongen, B.E., Semiletov, I.P., Dudarev, O. V., Yunker, M.B., MacDonald, R.W., Montluçon, D.B., Eglinton, T.I., 2015. Multi-molecular tracers of terrestrial carbon transfer across the pan-Arctic: Comparison of hydrolyzable components with plant wax lipids and lignin phenols. Biogeosciences 12, 4841–4860. doi:10.5194/bg-12-4841-2015

Ficken, K.J., Li, B., Swain, D.L., Eglinton, G., 2000. An n-alkane proxy for the sedimentary input of submerged/floating freshwater aquatic macrophytes. Org. Geochem. 31, 745–749. doi:10.1016/S0146-6380(00)00081-4

Galy, V., Eglinton, T., France-Lanord, C., Sylva, S., 2011. The provenance of vegetation and environmental signatures encoded in vascular plant biomarkers carried by the Ganges-Brahmaputra rivers. Earth Planet. Sci. Lett. 304, 1–12. doi:10.1016/j.epsl.2011.02.003

Galy, V., Peucker-Ehrenbrink, B., Eglinton, T., 2015. Global carbon export from the terrestrial biosphere controlled by erosion. Nature 521, 204–207. doi:10.1038/nature14400

Glendell, M., Brazier, R.E., 2014. Accelerated export of sediment and carbon from a landscape under intensive agriculture. Sci. Total Environ. 476–477, 643–656. doi:10.1016/j.scitotenv.2014.01.057

Glendell, M., Extence, C., Chadd, R., Brazier, R.E., 2014a. Testing the pressure-specific invertebrate index (PSI) as a tool for determining ecologically relevant targets for reducing sedimentation in streams. Freshw. Biol. 59, 353–367. doi:10.1111/fwb.12269

Glendell, M., Granger, S.J., Bol, R., Brazier, R.E., 2014b. Quantifying the spatial variability of soil physical and chemical properties in relation to mitigation of diffuse water pollution. Geoderma 214–215, 25–41.

Graeber, D., Goyenola, G., Meerhoff, M., Zwirnmann, E., Ovesen, N.B.B., Glendell, M., Gelbrecht, J., Teixeira de Mello, F., González-Bergonzoni, I., Jeppesen, E., Kronvang, B., 2015. Interacting effects of climate and agriculture on fluvial DOM in temperate and subtropical catchments. Hydrol. Earth Syst. Sci. 19, 2377–2394. doi:10.5194/hess-19-

2377-2015

Guzman, G., Quinton, J.N., Nearing, M.A., Mabit, L., G0mez, J.A., 2013. Sediment tracers in water erosion studies: Current approaches and challenges. J. Soils Sediments 13, 816–833. doi:10.1007/s11368-013-0659-5

Hamilton, S.K., Lewis, W.M., 1992. Stable carbon and nitrogen isotopes in algae and detritus from the Orinoco River floodplain, Venezuela. Geochim. Cosmochim. Acta 56, 4237–4246.

Laceby, J.P., Olley, J., Pietsch, T.J., Sheldon, F., Bunn, S.E., 2015. Identifying subsoil sediment sources with carbon and nitrogen stable isotope ratios. Hydrol. Process. 29, 1956–1971. doi:10.1002/hyp.10311

Lauerwald, R., Laruelle, G.G., Hartmann, J., Ciais, P., Regnier, P.A.G., 2015. Global Biogeochemical Cycles 534–554. doi:10.1002/2014GB004941.Received

Li, M., Peng, C., Wang, M., Xue, W., Zhang, K., Wang, K., Shi, G., Zhu, Q., 2017. The carbon flux of global rivers: A re-evaluation of amount and spatial patterns. Ecol. Indic. 80, 40–51. doi:10.1016/j.ecolind.2017.04.049

Ludwig, W., P. Amiotte-Suchet, J.L. Probst, F.G. Hall, G.J. Collatz, B.W. Meeson, S.O. Los, E.Brown De Colstoun, and D.R.L., 2011. ISLSCP II Global River Fluxes of Carbon and Sediments to the Oceans.

Maavara, T., Lauerwald, R., Regnier, P., Van Cappellen, P., 2017. Global perturbation of organic carbon cycling by river damming. Nat. Commun. 8, 15347. doi:10.1038/ncomms15347

Mackereth, F.J.H., 1969. Short core sampler for subaqueous deposits. Limnol. Oceanogr. 14, 145–151.

Marín-Spiotta, E., Gruley, K.E., Crawford, J., Atkinson, E.E., Miesel, J.R., Greene, S., Cardona-Correa, C., Spencer, R.G.M., 2014. Paradigm shifts in soil organic matter research affect interpretations of aquatic carbon cycling: Transcending disciplinary and ecosystem boundaries. Biogeochemistry 117, 279–297. doi:10.1007/s10533-013-9949-7

Meyers, P.A., Lallier-Vergès, E., 1999. Lacustrine sedimentary organic matter of Late Quaternary paleoclimates. J. Paleolimnol. 21, 345–372. doi:10.1023/A:1008073732192

Meyers, P. a, 2003. Application of organic geochemistry to paleolimnological reconstruction: a summary of examples from the Laurention Great Lakes. Org. Geochem. 34, 261–289.

Mouchet, M.A., Paracchini, M.L., Schulp, C.J.E., Sturck, J., Verkerk, P.J., Verburg, P.H., Lavorel, S., 2016. Bundles of ecosystem (dis) services and multifunctionality across European landscapes. Ecol. Indic. 73, 23–28. doi:10.1016/j.ecolind.2016.09.026. 73

Nakayama, T., 2017. Development of an advanced eco-hydrologic and biogeochemical coupling model aimed at clarifying the missing role of inland water in the global biogeochemical cycle. J. Geophys. Res. Biogeosciences.

Norris, C.E., Dungait, J.A.J., Joynes, A., Quideau, S.A., 2013. Biomarkers of novel ecosystem development in boreal forest soils. Org. Geochem. 64, 9–18.

Owens, P.N., Blake, W.H., Gaspar, L., Gateuille, D., Koiter, A.J., Lobb, D.A., Petticrew, E.L., Reiffarth, D.G., Smith, H.G., Woodward, J.C., 2016. Earth-Science Reviews Fingerprinting and tracing the sources of soils and sediments : Earth and ocean science , geoarchaeological , forensic , and human health applications. Earth Sci. Rev. 162, 1–23. doi:10.1016/j.earscirev.2016.08.012

Palazón, L., Latorre, B., Gaspar, L., Blake, W.H., Smith, H.G., Navas, A., 2015. Comparing catchment sediment fingerprinting procedures using an auto-evaluation approach with virtual sample mixtures. Sci. Total Environ. 532, 456–466. doi:10.1016/j.scitotenv.2015.05.003

Panagos, P., Borrelli, P., Poesen, J., Ballabio, C., Lugato, E., Meusburger, K., Montanarella, L., Alewell, C., 2015. The new assessment of soil loss by water erosion in Europe. Environ. Sci. Policy 54, 438–447. doi:10.1016/j.envsci.2015.08.012

Parnell, A., Jackson, A., 2008. Stable Isotope Analysis in R [WWW Document]. URL https://cran.r-project.org/package=siar

Puttock, A., Dungait, J.A.J., Macleod, C.J.A., Bol, R., Brazier, R.E., 2014. Woody plant encroachment into grasslands leads to accelerated erosion of previously stable organic carbon from dryland soils. J. Geophys. Res. Biogeosciences 119, 2345–2357. doi:10.1002/2014JG002635.Received

Ranjan, R.K., Routh, J., Val Klump, J., Ramanathan, A.L., 2015. Sediment biomarker profiles trace organic matter input in the Pichavaram mangrove complex, southeastern India. Mar. Chem. 171, 44–57. doi:10.1016/j.marchem.2015.02.001

Raymond, P. a, Hartmann, J., Lauerwald, R., Sobek, S., McDonald, C., Hoover, M., Butman, D., Striegl, R., Mayorga, E., Humborg, C., Kortelainen, P., Dürr, H., Meybeck, M., Ciais, P., Guth, P., 2013. Global carbon dioxide emissions from inland waters. Nature 503, 355–9. doi:10.1038/nature12760

Regnier, P., Friedlingstein, P., Ciais, P., Mackenzie, F.T., Gruber, N., Janssens, I. a., Laruelle, G.G., Lauerwald, R., Luyssaert, S., Andersson, A.J., Arndt, S., Arnosti, C., Borges, A. V., Dale, A.W., Gallego-Sala, A., Goddéris, Y., Goossens, N., Hartmann, J., Heinze, C., Ilyina, T., Joos, F., LaRowe, D.E., Leifeld, J., Meysman, F.J.R., Munhoven, G., Raymond, P. a., Spahni, R., Suntharalingam, P., Thullner, M., 2013. Anthropogenic perturbation of the carbon fluxes from land to ocean. Nat. Geosci. 6, 597–607. doi:10.1038/ngeo1830

Reiffarth, D.G., Petticrew, E.L., Owens, P.N., Lobb, D.A., 2016. Sources of variability in fatty acid (FA) biomarkers in the application of compound-specific stable isotopes (CSSIs) to soil and sediment fingerprinting and tracing: A review. Sci. Total Environ. 565, 8–27. doi:10.1016/j.scitotenv.2016.04.137

Rickson, R.J., 2014. Can control of soil erosion mitigate water pollution by sediments? Sci. Total Environ. 468–469, 1187–1197. doi:10.1016/j.scitotenv.2013.05.057

Schmidt, M.W.I., Torn, M.S., Abiven, S., Dittmar, T., Guggenberger, G., Janssens, I. a., Kleber, M., Kögel-Knabner, I., Lehmann, J., Manning, D. a. C., Nannipieri, P., Rasse, D.P., Weiner, S., Trumbore, S.E., 2011. Persistence of soil organic matter as an ecosystem property. Nature 478, 49–56. doi:10.1038/nature10386

306 Schoumans, O.F., Chardon, W.J., Bechmann, M.E., Gascuel-Odoux, C., Hofman, G.,
307 Kronvang, B., Rubæk, G.H., Ulén, B., Dorioz, J.M., 2014. Mitigation options to reduce
308 phosphorus losses from the agricultural sector and improve surface water quality: A
309 review. Sci. Total Environ. 468–469, 1255–1266. doi:10.1016/j.scitotenv.2013.08.061

310 Schroter, D., Cramer, W., Leemans, R., Arnell, N.W., Prentice, I.C., Arau, M.B., Bondeau,
311 A., Bugmann, H., Carter, T.R., Gracia, C.A., Vega-leinert, A.C. De, Erhard, M., Ewert,
312 F., Glendining, M., House, J.I., Klein, R.J.T., Lavorel, S., Kankaanpa, S., Lindner, M.,
313 Metzger, M.J., Meyer, J., Mitchell, T.D., Reginster, I., Rounsevell, M., 2005. Ecosystem
314 Service Supply and Vulnerability to Global Change in Europe.

315 Senbayram, M., Dixon, L., Goulding, K.W.T., B.R., 2008. Long-term influence of manure
316 and mineral nitrogen applications on plant and soil 15N and 13C values from the
317 Broadbalk Wheat Experiment. Rapid Commun. Mass Spectrom. 22, 1735–1740.
318 doi:10.1002/rcm.3548

319 Sherriff, S.C., Franks, S.W., Rowan, J.S., Fenton, O., Daire, Ó., 2015. Uncertainty-based
320 assessment of tracer selection , tracer non-conservativeness and multiple solutions in
321 sediment fingerprinting using synthetic and field data 2101–2116. doi:10.1007/s11368-
322 015-1123-5

323 Silliman, J.E., Schelske, C.L., 2003. Saturated hydrocarbons in the sediments of Lake
324 Apopka, Florida. Org. Geochem. 34, 253–260. doi:10.1016/S0146-6380(02)00169-9

325 Smith, H.G., Evrard, O., Blake, W.H., Owens, P.N., Smith, H.G., 2015. Preface —
326 Addressing challenges to advance sediment fingerprinting research 2033–2037.
327 doi:10.1007/s11368-015-1231-2

328 Tao, S., Eglinton, T.I., Montluçon, D.B., McIntyre, C., Zhao, M., 2016. Diverse origins and
329 pre-depositional histories of organic matter in contemporary Chinese marginal sea
330 sediments. Geochim. Cosmochim. Acta 191, 70–88. doi:10.1016/j.gca.2016.07.019

331 Team, R.C., 2014. R: A language and environment for statistical computing. R Foundation
332 for Statistical Computing, Vienna, Austria.

333 Tian, H., 2015. Journal of Geophysical Research: Biogeosciences. J. Geophys. Res.
334 Biogeosciences 120, 752–772. doi:10.1002/2014JG002760.Received

335 Tilman, D., Cassman, K.G., Matson, P.A., Naylor, R., Polasky, S., 2002. Agricultural
336 sustainability and intensive production practices. Nature 418, 671–677.
337 doi:10.1038/nature01014

338 Tolosa, I., Fiorini, S., Gasser, B., Martín, J., Miquel, J.C., 2013. Carbon sources in suspended
339 particles and surface sediments from the Beaufort Sea revealed by molecular lipid
340 biomarkers and compound-specific isotope analysis. Biogeosciences 10, 2061–2087.
341 doi:10.5194/bg-10-2061-2013

342 Torres, T., Ortiz, J.E., Martin-Sanchez, D., Arribas, I., Moreno, L., Ballesteros, B., Blazquez,
343 A., Dominguez, J.A., Estrealla, T.R., 2014. The long Pleistocene record from the Pero-
344 Oliva marshland (Alicante-Valencia, Spain), in: Martini, I.P., Wanless, H.R. (Ed.),
345 Sedimentary Coastal Zones from High to Low Latitudes: Similarities and Differences.
346 Geological Society of London, pp. 429–448.

Tranvik, L.J., Downing, J.A., Cotner, J.B., Loiselle, S.A., Striegl, R.G., Ballatore, T.J., Dillon, P., Finlay, K., Fortino, K., Knoll, L.B., Kortelainen, P.L., Kutser, T., Larsen, S., Laurion, I., Leech, D.M., McCallister, S.L., McKnight, D.M., Melack, J.M., Overholt, E., Porter, J.A., Prairie, Y., Renwick, W.H., Roland, F., Sherman, B.S., Schindler, D.W., Sobek, S., Tremblay, A., Vanni, M.J., Verschoor, A.M., von Wachenfeldt, E., Weyhenmeyer, G.A., 2009. Lakes and reservoirs as regulators of carbon cycling and climate. Limnol. Oceanogr. 54, 2298–2314. doi:10.4319/lo.2009.54.6_part_2.2298

Turnage, K.M., Lee, S.Y., Foss, J.E., Kim, K.H., Larsen, I.J., 1997. Comparison of soil erosion and deposition rates using radiocesium, RUSLE, and buried soils in dolines in East Tennessee. Environ. Geol. 29, 1–10.

Verheijen, F.G.A., Jones, R.J.A., Rickson, R.J., Smith, C.J., 2009. Tolerable versus actual soil erosion rates in Europe. Earth-Science Rev. 94, 23–38. doi:10.1016/j.earscirev.2009.02.003

Walling, D.E., 2013. The evolution of sediment source fingerprinting investigations in fluvial systems. J. Soils Sediments 13, 1658–1675. doi:10.1007/s11368-013-0767-2

Wohl, E., Hall, R.O., Lininger, K.B., Sutfin, N.A., Walters, D.M., 2017. Carbon dynamics of river corridors and the effects of human alterations. Ecol. Monogr. 87, 379–409. doi:10.1002/ecm.1261

Zech, M., Krause, T., Meszner, S., Faust, D., 2013. Incorrect when uncorrected: Reconstructing vegetation history using n-alkane biomarkers in loess-paleosol sequences - A case study from the Saxonian loess region, Germany. Quat. Int. 296, 108–116. doi:10.1016/j.quaint.2012.01.023

Zech, M., Rass, S., Buggle, B., L??scher, M., Z??ller, L., 2012. Reconstruction of the late Quaternary paleoenvironments of the Nussloch loess paleosol sequence, Germany, using n-alkane biomarkers. Quat. Res. (United States) 78, 226–235. doi:10.1016/j.yqres.2012.05.006

Zech, M., Zech, R., Morr??s, H., Moretti, L., Glaser, B., Zech, W., 2009. Late Quaternary environmental changes in Misiones, subtropical NE Argentina, deduced from multi-proxy geochemical analyses in a palaeosol-sediment sequence. Quat. Int. 196, 121–136. doi:10.1016/j.quaint.2008.06.006

Zhang, X.C. (John), Liu, B.L., 2016. Using multiple composite fingerprints to quantify fine sediment source contributions: A new direction. Geoderma 268, 108–118. doi:10.1016/j.geoderma.2016.01.031

Appendix 1 n-alkane data

			n-alkane concentration µg g^{-1} soil																	
Landuse	Source	Code*	C15	C16	C17	C18	C19	C20	C21	C22	C23	C24	C25	C26	C27	C28	C29	C30	C31	C32	C33
grass	soil	1.1	0.36	0.50	0.32	0.61	n/a	0.28	0.38	0.46	0.32	0.26	0.66	0.16	1.49	0.33	3.79	0.59	6.30	0.32	3.82
grass	soil	1.2	0.36	0.87	0.55	0.77	n/a	0.43	0.71	0.38	0.38	0.18	0.82	0.36	1.61	0.50	3.93	0.57	6.63	0.35	3.85
grass	soil	1.3	0.57	0.50	0.37	0.59	n/a	0.69	0.58	0.19	0.06	0.05	0.62	0.08	1.17	0.24	4.31	0.51	7.32	0.18	4.19
grass	soil	1.4	0.18	0.27	0.23	0.37	n/a	0.40	0.35	0.19	0.27	0.28	0.38	0.03	0.73	0.48	2.20	0.34	4.13	0.25	2.15
grass	soil	1.5	0.07	0.19	0.16	0.50	n/a	0.34	0.34	0.23	0.53	0.17	0.75	0.37	1.53	0.55	2.98	0.61	5.29	0.45	3.37
arable	soil	2.1	0.28	0.33	0.29	0.56	n/a	0.82	0.40	0.15	0.09	0.39	0.37	0.09	1.28	0.27	2.37	0.35	3.81	0.24	1.98
arable	soil	2.2	0.09	0.08	0.09	0.27	n/a	0.19	0.21	0.17	0.28	0.11	0.39	0.14	0.84	0.24	2.13	0.34	3.65	0.23	1.99
arable	soil	2.3	0.11	0.28	0.24	0.43	n/a	0.42	0.26	0.12	0.30	0.18	0.38	0.19	0.90	0.25	2.00	0.38	3.71	0.23	2.00

arable	soil	2.4	0.08	0.10	0.12	0.26	n/a	0.31	0.17	0.10	0.30	0.18	0.43	0.18	1.08	0.28	1.93	0.27	3.34	0.24	1.81
arable	soil	3.3	0.08	0.09	0.11	0.24	n/a	0.21	0.26	0.10	0.27	0.20	0.61	0.19	1.57	0.37	3.02	0.40	4.33	0.26	2.30
woodland	soil	3.4	0.31	0.58	0.58	0.99	n/a	2.42	2.17	0.17	1.76	1.20	4.28	0.65	20.68	1.89	20.42	1.38	11.48	0.69	7.87
ley	soil	5.2	0.40	0.49	0.59	0.96	n/a	2.34	1.91	0.47	0.38	1.04	2.20	0.20	0.49	3.22	3.81	0.70	6.21	0.44	1.49
ley	soil	5.3	0.85	0.98	0.99	1.52	n/a	3.28	3.08	0.29	2.29	0.40	1.79	1.27	1.82	1.39	3.37	0.46	5.50	0.35	2.60
ley	soil	5.4	0.25	0.23	0.29	0.48	n/a	2.03	0.99	0.28	0.14	0.37	0.17	0.36	1.98	3.27	4.01	0.80	5.68	0.46	2.99
ley	soil	5.5	0.05	0.12	0.14	0.25	n/a	0.21	0.46	0.12	0.52	0.30	1.48	0.78	2.59	1.33	5.04	1.13	6.98	0.58	3.75
ley	soil	6.4	0.08	0.12	0.15	0.29	n/a	0.20	0.24	0.09	0.21	0.25	0.57	0.26	1.48	0.45	3.08	0.58	5.14	0.40	2.84
ley	soil	6.5	0.09	0.21	0.20	0.37	n/a	0.20	0.22	0.05	0.19	0.08	0.49	0.26	1.20	0.47	2.67	0.56	4.13	0.29	2.32
woodland	soil	6.6	0.06	0.11	0.14	0.35	n/a	0.28	0.44	0.64	1.19	0.96	3.48	1.48	14.55	2.01	15.31	1.09	7.12	0.65	3.48
grass	soil	8.5	0.1	0.1	0.1	0.2	n/a	0.1	0.1	0.1	0.1	0.2	0.6	0.3	1.71	0.8	3.14	0.7	4.78	0.3	2.1

			5	4	3	1		6	9	1	9	8	4	7		5		7		6	4
arable	soil	9.1	0.07	0.17	0.13	0.29	n/a	0.28	0.12	0.06	0.18	0.09	0.52	0.13	1.05	0.37	3.15	0.45	5.66	0.33	3.03
woodland	soil	9.7	0.04	0.04	0.05	0.09	n/a	0.13	0.28	0.16	0.48	0.30	2.07	0.60	10.70	1.34	9.02	0.60	4.97	0.33	4.57
arable	soil	10.5	0.07	0.12	0.14	0.35	n/a	0.24	0.25	0.17	0.11	0.10	0.32	0.07	0.77	0.18	1.71	0.26	2.83	0.18	1.41
ley	soil	11.5	0.27	0.26	0.18	0.34	n/a	0.49	0.41	0.13	0.14	0.13	0.08	0.14	0.44	0.13	1.54	0.18	2.72	0.14	1.08
ley	soil	11.6	0.07	0.08	0.11	0.25	n/a	0.22	0.24	0.19	0.11	0.05	0.57	0.06	0.69	0.21	2.10	0.25	3.57	0.18	1.67
ley	soil	11.7	0.21	0.12	0.19	0.31	n/a	0.84	0.72	0.05	0.19	0.33	0.14	0.18	0.88	0.23	2.23	0.51	3.21	0.22	1.22
grass	soil	11.8	0.11	0.03	0.05	0.18	n/a	0.19	0.45	0.18	0.66	0.56	1.43	0.66	4.75	0.90	6.35	0.68	4.21	0.30	1.65
woodland	soil	12.5	0.04	0.08	0.11	0.18	n/a	2.19	0.86	0.06	0.25	0.31	2.09	0.94	5.79	0.13	10.81	1.08	6.01	0.47	1.67
arable	soil	13.3	0.18	0.23	0.30	0.56	n/a	1.27	1.37	0.15	0.29	0.10	0.25	0.46	0.32	0.68	3.02	0.48	4.75	0.28	2.50
arable	soil	13.4	0.39	0.56	0.45	0.92	n/a	2.23	2.46	0.54	0.43	0.95	0.50	0.09	1.01	1.42	6.18	0.16	4.46	0.24	1.76

arable	soil	13.5	0.24	0.31	0.38	0.67	n/a	1.20	1.21	0.15	0.14	0.12	0.46	0.08	0.84	0.61	2.25	0.33	3.51	0.21	1.68
arable	soil	13.6	0.15	0.10	0.16	0.37	0.14	0.26	0.45	0.23	0.07	0.15	0.17	0.11	0.54	0.09	1.74	0.16	2.39	0.18	1.40
river	upstream	4	0.16	0.04	0.05	0.13	0.05	0.16	0.08	0.18	0.17	0.14	0.59	0.17	2.25	0.21	2.20	0.19	0.90	0.06	0.31
river	midstream	6	0.12	0.09	0.09	0.32	0.26	0.33	1.14	0.32	0.27	0.27	1.25	0.35	5.61	0.47	5.50	0.12	2.13	0.17	0.82
river	downstream	7	0.09	0.07	0.10	0.23	0.19	0.25	0.31	0.14	0.55	0.28	1.99	0.34	8.09	0.74	7.48	0.53	3.10	0.14	1.17
river	upstream	9	0.25	0.12	0.52	0.65	0.26	0.26	0.89	0.20	0.29	0.30	1.22	0.31	5.15	0.49	6.13	0.56	2.95	0.24	1.01
river	midstream	11	0.20	0.07	0.11	0.24	0.23	0.28	0.36	0.12	0.73	0.26	2.01	0.70	8.57	1.07	9.43	0.65	4.32	0.12	1.78
river	downstream	13	0.69	0.24	0.52	0.71	0.19	0.18	0.15	0.17	0.21	0.37	1.05	0.06	5.18	0.20	5.95	0.44	2.53	0.26	0.89
river	outlet	OUT	0.15	0.09	0.27	0.50	0.33	0.33	0.29	0.35	0.36	0.71	1.33	0.20	5.07	0.10	4.75	0.35	2.63	0.21	1.75
lake	1	0-4 cm	0.10	0.49	0.72	0.70	0.59	0.26	0.64	0.33	1.54	0.61	3.88	0.85	18.94	1.18	17.34	1.15	9.14	0.45	6.75
lake	2	4-8 cm	0.5	0.4	1.1	0.9	0.3	0.5	0.5	0.6	0.9	1.1	5.2	1.3	20.4	1.0	20.3	2.6	12.3	0.3	4.7

			4	5	7	3	4	6	4	5	7	8	4	9	8	6	0	6	9	1	5
lake	3	8-12 cm	0.16	0.50	1.04	0.87	0.98	0.33	1.05	0.42	1.43	0.57	4.96	0.75	19.02	0.31	18.59	1.29	11.52	0.27	6.18
lake	4	12-16 cm	0.31	0.33	0.43	0.70	0.54	0.08	0.62	1.03	1.20	2.86	5.15	0.89	21.97	0.13	20.74	0.50	14.39	0.16	5.70
lake	5	16-20 cm	0.13	0.44	0.66	0.60	1.09	1.51	1.14	0.36	2.23	0.46	4.76	0.64	17.27	2.15	17.82	1.59	12.40	1.03	4.12
lake	6	20-24 cm	0.42	0.48	0.70	0.62	0.72	3.16	1.97	0.39	2.73	2.91	0.57	0.80	15.72	0.80	16.11	0.44	12.85	0.05	6.58
lake	7	24-28 cm	0.11	0.31	0.70	1.06	1.62	3.35	1.50	0.22	3.52	0.40	4.60	1.16	16.68	3.97	15.78	0.45	12.32	1.38	4.47
lake	8	28-32 cm	0.41	0.59	1.27	1.05	1.16	2.07	0.81	1.00	2.03	3.94	4.50	0.17	17.21	2.26	15.36	0.45	12.09	0.99	3.55
lake	9	32-36 cm	0.56	0.82	1.96	1.58	1.21	1.85	0.89	1.26	1.98	3.87	5.62	0.63	18.99	0.59	17.77	0.89	12.82	0.79	4.03
lake	10	36-40 cm	0.19	0.38	3.54	0.75	1.68	0.16	1.04	0.40	1.58	1.21	4.69	1.05	13.60	3.25	15.73	1.36	13.10	0.77	5.80
lake	11	40-44 cm	0.03	0.12	1.49	0.31	0.62	0.50	0.53	0.20	1.47	1.35	2.45	0.56	7.07	1.52	9.95	0.93	9.05	0.43	2.97
lake	12	44-48 cm	0.20	0.27	1.67	1.10	1.00	1.66	0.78	0.56	2.08	1.38	3.62	0.78	10.42	3.23	13.88	1.06	12.88	0.54	4.33

*	transect and core number for soil samples
	location for stream bed sediment samples
	depth increment for lake core

Appendix 2 – stable isotope data

Landuse	Source	Code	% N	$\delta^{15}N$ ‰	% C	$\delta^{13}C$ ‰
grass	soil	1.1	0.42	5.20	4.12	-27.81
grass	soil	1.2	0.49	5.78	5.53	-27.27
grass	soil	1.3	0.57	3.26	6.50	-28.33
grass	soil	1.4	0.44	6.37	4.13	-27.34
grass	soil	1.5	0.61	6.66	6.02	-28.02
arable	soil	2.1	0.40	4.81	4.14	-27.01
arable	soil	2.2	0.30	3.72	2.99	-28.00
arable	soil	2.3	0.38	7.59	3.99	-27.00
arable	soil	2.4	0.37	5.05	3.55	-26.98
arable	soil	3.1	0.39	4.97	3.56	-27.85
arable	soil	3.2	0.37	5.93	3.66	-27.05
arable	soil	3.3	0.25	4.80	2.57	-27.69
woodland	soil	3.4	0.84	5.56	10.36	-28.11
woodland	soil	3.4b	0.69	5.63	8.76	-27.71
woodland	soil	3.4c	0.49	4.70	6.92	-28.35
ley	soil	4.1	0.36	5.07	3.35	-28.27
ley	soil	4.2	0.41	5.35	4.08	-28.13
ley	soil	4.3	0.47	5.25	4.78	-28.30
ley	soil	4.4	0.43	5.09	4.10	-28.43
ley	soil	5.1	0.41	5.10	4.17	-27.95
ley	soil	5.2	0.40	5.28	3.69	-28.37
ley	soil	5.3	0.41	5.69	4.09	-28.01
ley	soil	5.4	0.43	5.20	4.19	-28.52

ley	soil	5.5	0.57	4.90	5.87	-28.58
ley	soil	6.1	0.35	4.87	3.15	-27.99
ley	soil	6.2	0.32	3.82	3.00	-28.72
ley	soil	6.3	0.33	4.63	3.02	-28.14
ley	soil	6.4	0.40	4.85	3.75	-28.41
ley	soil	6.5	0.44	3.96	4.18	-28.52
woodland	soil	6.6	0.64	5.58	7.16	-28.65
arable	soil	7.1	0.35	5.53	3.25	-27.26
arable	soil	7.2	0.21	5.39	1.83	-27.29
ley	soil	7.3	0.23	5.69	2.20	-26.96
ley	soil	7.4	0.31	6.07	2.70	-27.47
ley	soil	7.5	0.38	5.71	3.52	-27.88
grass	soil	7.6	0.59	6.27	5.56	-28.28
grass	soil	7.7	0.48	7.07	5.10	-28.14
ley	soil	8.1	0.47	5.86	4.60	-28.28
ley	soil	8.2	0.38	6.79	3.42	-28.17
arable	soil	8.3	0.32	6.11	2.78	-27.29
arable	soil	8.4	0.32	5.53	2.92	-27.42
grass	soil	8.5	0.68	5.20	6.73	-28.38
grass	soil	8.6	0.71	4.16	6.88	-28.33
arable	soil	9.1	0.35	5.07	3.40	-27.78
arable	soil	9.2	0.32	5.90	2.90	-28.19
grass	soil	9.3	0.92	7.29	8.28	-29.15
grass	soil	9.4	0.60	4.99	5.77	-28.42
grass	soil	9.5	0.48	5.33	4.48	-28.38
grass	soil	9.6	0.47	6.24	4.45	-27.62

woodland	soil	9.7	0.50	5.94	4.98	-28.51
ley	soil	10.1	0.38	6.89	3.22	-28.42
arable	soil	10.2	0.31	6.38	2.64	-27.26
arable	soil	10.3	0.35	5.43	2.90	-27.56
arable	soil	10.4	0.27	5.39	2.34	-27.86
arable	soil	10.5	0.34	4.95	2.98	-27.82
woodland	soil	10.6	0.77	3.80	9.59	-28.25
arable	soil	11.1	0.22	3.62	2.08	-27.85
arable	soil	11.3	0.31	5.20	2.72	-28.00
arable	soil	11.4	0.35	5.17	2.89	-27.84
ley	soil	11.5	0.28	5.95	2.12	-27.69
ley	soil	11.6	0.37	6.01	3.45	-28.09
ley	soil	11.7	0.32	5.33	2.56	-27.79
grass	soil	11.8	0.43	4.10	4.80	-28.84
ley	soil	12.1	0.43	7.64	3.67	-28.82
ley	soil	12.3	0.41	6.66	3.56	-28.46
ley	soil	12.4	0.38	6.03	3.06	-28.23
woodland	soil	12.5	0.50	1.77	8.68	-28.02
arable	soil	13.1	0.31	6.09	2.64	-27.74
arable	soil	13.2	0.38	6.52	3.36	-27.87
arable	soil	13.3	0.30	6.24	2.56	-28.13
arable	soil	13.4	0.29	5.38	2.46	-27.65
arable	soil	13.5	0.29	4.39	2.25	-27.95
arable	soil	13.6	0.32	5.91	2.63	-27.69
arable	soil	14.1	0.29	5.57	2.24	-27.84
arable	soil	14.2	0.31	5.59	2.73	-27.74

arable	soil	14.3	0.34	5.71	2.95	-27.04
arable	soil	14.4	0.37	6.12	3.28	-27.18
arable	soil	14.5	0.38	6.40	3.47	-28.00
river	Upstream	4	0.11	3.41	1.16	-28.15
river	Midstream	6	0.16	3.34	2.08	-28.23
river	Downstream	7	0.21	4.98	2.74	-28.71
river	Upstream	9	0.24	6.48	2.82	-28.34
river	Midstream	11	0.28	4.63	3.68	-28.28
river	Downstream	13	0.19	4.45	2.32	-28.33
river	outlet	OUT	0.13	4.52	1.55	-27.91
lake	0-2 cm	1_1	0.76	6.58	8.32	-28.16
lake	0-2 cm	1_1	0.75	6.31	8.44	-28.20
lake	2-4 cm	1_1	0.76	6.68	8.46	-28.18
lake	4-6 cm	1_2	0.72	6.28	7.84	-28.27
lake	6-8 cm	1_3	0.66	5.76	7.71	-28.24
lake	8-10 cm	1_4	0.69	6.26	7.85	-27.99
lake	10-12 cm	1_5	0.67	6.36	7.53	-28.04
lake	12-14 cm	1_6	0.69	6.17	7.41	-27.99
lake	14-16 cm	1_7	0.68	6.90	7.37	-27.97
lake	16-18 cm	1_8	0.69	6.72	7.65	-27.96
lake	18-20 cm	1_9	0.78	6.94	9.40	-27.73
lake	22-24 cm	1_10	0.77	6.69	9.15	-27.21
lake	24-26 cm	1_11	0.80	6.78	8.50	-27.23
lake	26-28 cm	1_12	0.72	6.33	7.66	-27.33
lake	28-30 cm	1_13	0.78	6.25	8.41	-27.09
lake	32-34 cm	1_14	0.72	6.26	7.58	-27.16

lake	34-36 cm	1_15	0.74	6.63	7.75	-27.15
lake	36-38 cm	1_16	0.73	6.87	7.74	-27.19
lake	38-40 cm	1_17	0.65	6.05	7.06	-27.44
lake	40-42 cm	1_18	0.63	6.58	6.58	-27.68
lake	42-44 cm	1_19	0.57	5.94	5.95	-28.01
lake	44-46 cm	1_20	0.54	6.10	5.72	-27.83
lake	46-48 cm	1_21	0.61	5.88	6.39	-27.58
lake	48-50 cm	1_22	0.58	6.03	6.04	-27.35
lake	50-52 cm	1_23	0.56	6.06	5.51	-27.40
lake	52-54 cm	1_24	0.64	5.76	5.89	-26.86
lake	54-56 cm	1_25	0.62	5.73	5.80	-26.84